
Initial Experience with Technetium-99m HM-PAO Brain SPECT

I. Podreka, E. Suess, G. Goldenberg, M. Steiner, T. Brücke, Ch. Müller, W. Lang, R.D. Neirinckx, and L. Deecke

Abteilung für Neuronuklearmedizin der Neurologischen Universitätsklinik Wien, Vienna, Austria; and Amersham International, Buckinghamshire, United Kingdom

Technetium-99m-hexamethylpropyleneamineoxime (^{99m}Tc]HM-PAO) brain single photon emission computed tomography (SPECT) was performed with a dual head rotating scintillation camera. Normal tracer distribution and side/side differences of counting rates were obtained in 11 healthy volunteers. Almost stable gray/white matter ratios were found (1.97–2.1) in one normal subject during 2 hr after tracer administration. Eighty-three investigated patients had the following diagnoses (in parentheses is percent of positive findings in each group): cerebral vascular disease 18 (94.4%), epilepsy 23 (82.6%), extrapyramidal disorders 8 (100%), dementia 12 (100%), headache 11 (63.6%), psychiatric disorders 11 (27.3%). In addition, SPECT was performed in 28 male volunteers during motor or visual imagery tasks and a significant increase ($p = 0.035$) of relative tracer deposition was observed in the left inferior occipital region during visual imagery when compared with motor imagery. The results indicate that ^{99m}Tc]HM-PAO SPECT is valuable for demonstrating pathologic and physiologic changes of the brain.

J Nucl Med 28:1657–1666, 1987

In the past few years several technetium-labeled compounds that cross the blood-brain barrier (1) have been synthesized. Redistribution between gray and white matter and rapid washout limited their use only to dynamic brain single photon emission computed tomography (SPECT) (2). Technetium-99m hexamethylpropyleneamineoxime (^{99m}Tc]HM-PAO) developed recently by Amersham International (3) is a promising new ^{99m}Tc -labeled lipophilic agent with high first-pass extraction fraction (4) and deposition in the brain proportional to cerebral blood flow. The nearly constant maintenance of the regional distribution of ^{99m}Tc]HM-PAO over several hours, provides ideal conditions for equilibrium brain SPECT.

We report normal regional distribution of ^{99m}Tc]HM-PAO and our initial clinical experience using this tracer for visualization of rCBF changes in neurologic or psychiatric disorders. Furthermore, we compared SPECT results with those obtained by computed axial tomography (CAT) and investigated the possibility of applying ^{99m}Tc]HM-PAO to neuropsychologic stimulation studies.

Received Aug. 5, 1986; revision accepted May 11, 1987.

For reprints contact: Doz. Dr. Ivo Podreka, Neurologische Universitätsklinik Wien, Lazarettgasse 14, A-1090 Vienna, Austria.

MATERIAL AND METHODS

For SPECT studies 15–30 mCi of ^{99m}Tc]pertechnetate in 5 ml saline were added to a sealed glass vial, containing a freeze-dried formulation of the ligand HM-PAO and reductant, stannous tartrate, under an atmosphere of nitrogen gas. Following ligand preparation a solution of 12–20 mCi (444–740 MBq) of ^{99m}Tc]HM-PAO was withdrawn from the vial and injected 2–5 min later intravenously to the investigated subject. Sodium perchlorate (500 mg) was given before each ^{99m}Tc]HM-PAO administration.

A group of 11 male volunteers was scanned in the resting state for estimation of normal tracer distribution. In one healthy male volunteer six SPECT studies were obtained within 2 hr in order to investigate tracer redistribution. We investigated 83 patients with various neurologic or psychiatric diseases. In addition, SPECT studies were carried out in healthy male volunteers during a low imagery (14 subjects) and high imagery (14 subjects) task following written informed consent. SPECT was performed using a dual head rotating scintillation camera* and a dedicated computer system†. The subject was placed in a supine position on a dentist's chair with the head fixed in a thin cylindrical plastic head holder. The organ of interest, therefore, extended only to the lower half of the camera field. In this way the detectors cleared the patient's shoulders and the diameter of rotation was reduced to 250 mm. Thus, no modification of the camera heads (5) or usage of slant hole collimators (6) was needed to improve spatial resolution. Parallel hole collimators (LEAP, HRES, or

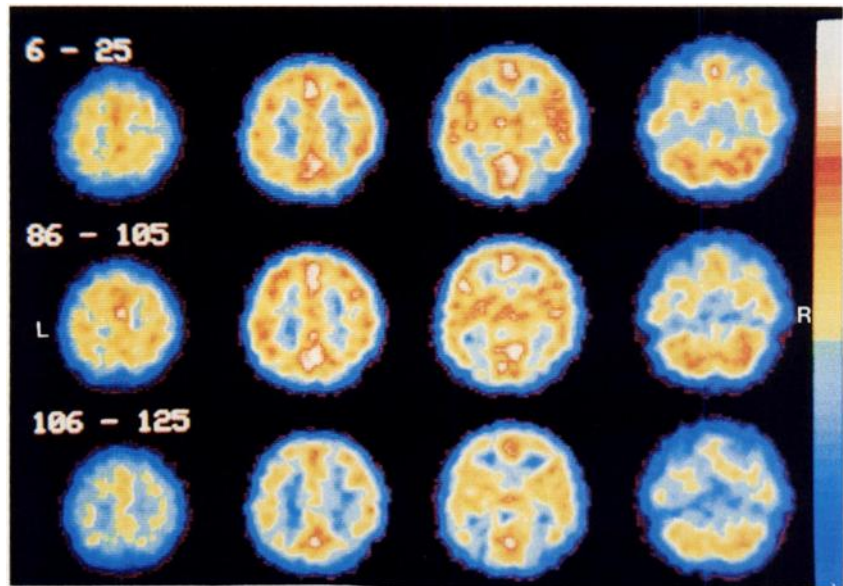


FIGURE 1

Adjacent transverse cross sections from cranial (left) to caudal (right) obtained from three out of six consecutive rotations within 2 hr (6–25, 86–105, and 106–125 min after tracer administration) in one normal subject. No substantial difference is seen between the 6–25 and 86–105 min images, while the 106–125 min images show a slight decrease in tracer concentration (LEAP collimators).

UHRES; FWHM: 14, 12, 9 mm in the horizontal plane) were used and 60 (2×30) projections were achieved within 30 min (60 sec/angle) with a linear sampling distance of 3.125 mm. Acquisition time was reduced to 20 min only once [estimation of tracer redistribution within 2 hr in one healthy subject (Fig. 1)]. Scanning was started 10 to 15 min after tracer administration. Usually 7 to 10 million counts were achieved from the projections. Image processing involved the prerecon-

structional filtering of angle views, using a weighted smooth filter of variable shape and size (7) for reduction of Poisson noise. A sinogram was created by reorganization of the corrected projections and 3.125-mm-thick transverse slices (128×128 matrices) were reconstructed by filtered backprojection (soft Shepp-Logan filter superimposed to a ramp filter with a cutoff frequency of 32 cycles/pixel). Each reconstructed slice was corrected for tissue absorption using Bellini's analytical

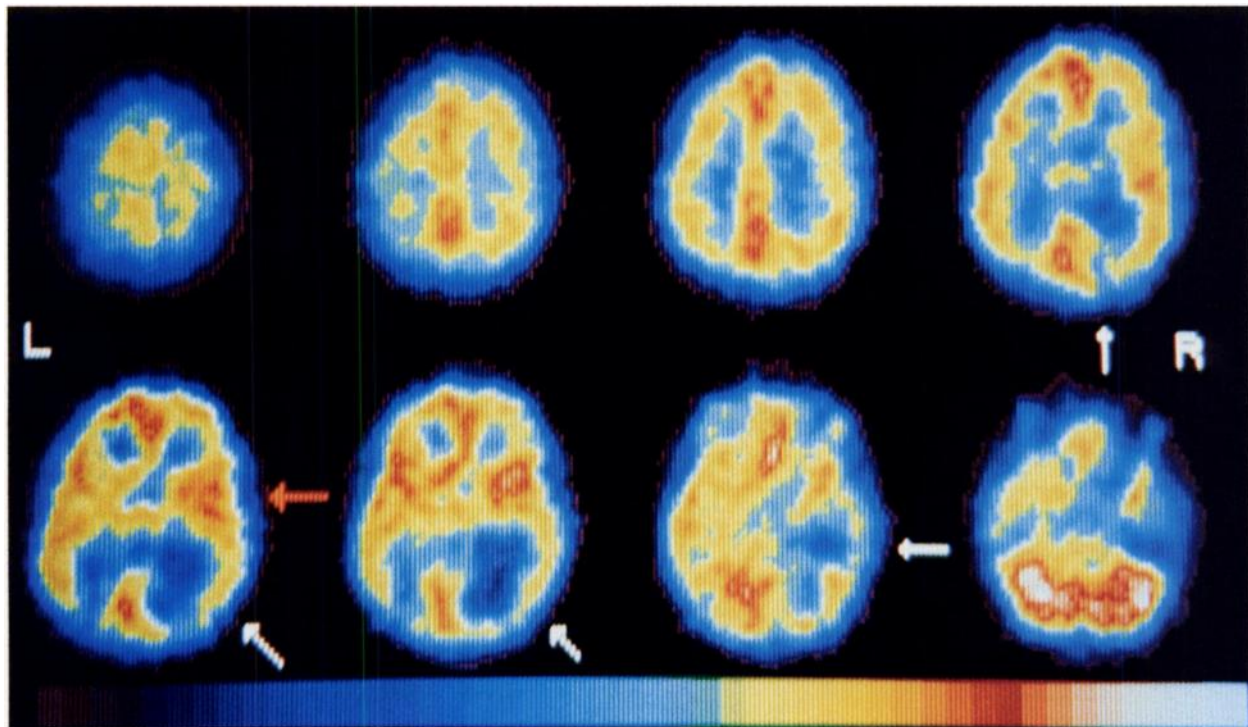


FIGURE 2

Transverse cross-sections (cranial = left; caudal = right) obtained in a 24-yr-old female patient with a RIND in the territory supplied by the right posterior cerebral artery. At onset left sided homonymous hemianopia along with headache was present. The study was performed 3 days after the insult. A low perfused region in the right occipital and temporal lobe is seen (white arrows). Relative hyperperfusion is visible in the right insula (red arrow). In a control study performed 14 days later when symptomatology cleared, no abnormality could be detected (LEAP collimators).

method (8) with a constant attenuation coefficient of 0.189/cm. All final cross-sections contained together 1 to 2 million counts. Five or seven cross-sections were summed consecutively to give a set of 15.6-mm or 21.9-mm-thick transverse slices (250,000 to 350,000 cts/slice) covering the entire organ for final evaluation. In particular, the prereconstructional filtering of projections (9,10) led to an improved delineation of anatomic detail in the images.

The clearance of [^{99m}Tc]HM-PAO from blood was reported by Sharp et al. (11). At 20', 40', 1 hr, and 2 hr postinjection the blood levels were 14%, 13%, 12%, and 11% of the injected dose, respectively. If the brain (1,400 ml) contains ~112 ml (=8% of 1,400 ml) of blood (CBV), the activity contribution by this small volume would be ~0.3%. Since the brain tissue itself traps ~5% of the injected dose [^{99m}Tc]HM-PAO SPECT images are largely flow-related. The proportion of the registered counts resulting from CBF and CBV would be ~17:1.

With absolute quantitation of [^{99m}Tc]HM-PAO SPECT studies not yet possible, side to side differences in brain isotope uptake were obtained by visual estimation and by calculation of left/right percentage differences in regions of interest (ROIs) larger than 2 × FWHM spatial resolution in the reconstructed images (12). Side to side differences above 12% were defined as abnormal based upon the data obtained in healthy subjects.

RESULTS

Normal Tracer Distribution

Normal regional tracer distribution and side to side differences in the resting state (closed eyes, fan background noise) were obtained in 11 healthy male volunteers (21–29 yr of age; mean 24 ± 2.9 yr). We calculated "regional indices" (RIs) [where RI = (mean cts/voxel of a ROI)/(mean cts/voxel of all ROIs)] in 15 regions of each hemisphere. Table 1 shows the RI values of each region and the difference of counts (in %) between homologous brain regions. Highest tracer uptake was found in the occipital and frontal lobes, followed by the anterior basal ganglia. Mean values of count differences ranged between 0.42 to 5.57% and s.d.s between 2.45 to 3.67%. The mean value ±2 s.d. for each region did not exceed 12%.

One 25-yr-old healthy male volunteer was scanned consecutively six times in 2 hr (20 min/SPECT study) in order to investigate the stability of temporal regional tracer distribution. The first SPECT study was begun 6 min after [^{99m}Tc]HM-PAO administration. Total counting rates remained almost constant between 6 and 85 min after tracer administration when corrected for isotope decay (first rotation: 915,640 cts = 100%; following rotations: 917,812 cts = 100.2%, 914,724 cts = 99.9%, 910,146 cts = 99.4%, 882,677 cts = 96.4%, 900,990 cts = 98.4%) whereas slight washout was observed after this time. Figure 1 displays equivalent transverse cross sections of the first, second, and sixth SPECT investigation. Regional tracer distribution remained constant with no redistribution between gray and white matter. Following gray/white matter ratios

TABLE 1
Mean Values ± s.d. of the "Regional Index" and Side/Side Differences of Counting Rates in % for 15 Homologous Regions of Each Hemisphere Obtained in 11 Healthy Male Volunteers*

Region	Hemisphere			Side/side %-Difference
	Left	RI	Right	
Upper ant. frontal	0.903 ± 0.036	0.924 ± 0.027	2.670 ± 3.412	
Med. ant. frontal	1.021 ± 0.024	1.036 ± 0.032	1.545 ± 2.750	
Inf. ant. frontal	1.051 ± 0.052	1.088 ± 0.033	4.166 ± 3.145	
Mid frontal	0.991 ± 0.022	1.018 ± 0.019	2.853 ± 2.554	
Inf. frontal + insula	1.043 ± 0.037	1.096 ± 0.040	5.328 ± 3.215	
Upper central	0.886 ± 0.037	0.877 ± 0.036	0.416 ± 3.489	
Lower central	0.952 ± 0.021	0.956 ± 0.039	2.710 ± 3.666	
Upper parietal	0.894 ± 0.040	0.921 ± 0.030	3.300 ± 2.454	
Inf. parietal	0.975 ± 0.020	0.996 ± 0.023	1.625 ± 3.587	
Sup. occipital	1.086 ± 0.028	1.105 ± 0.035	1.419 ± 3.127	
Inf. occipital	1.105 ± 0.042	1.126 ± 0.043	1.970 ± 3.030	
Sup. temporal	1.020 ± 0.031	1.049 ± 0.027	2.813 ± 2.641	
Inf. temporal	0.924 ± 0.032	0.976 ± 0.039	5.570 ± 3.112	
Ant. basal ganglia	1.043 ± 0.045	1.086 ± 0.052	4.578 ± 2.447	
Thalamus	0.998 ± 0.063	1.007 ± 0.036	1.208 ± 3.471	

* Regional Index (RI) of the whole brain = 1.0. The regions were drawn on four adjacent 21.9 mm thick transverse cross-sections.

for the six studies in 21.9-mm-thick transverse sections were found: 1.97, 2.0, 2.0, 1.99, 2.1, 2.0. Corresponding RIs varied from 1.3% to 5.3% (mean 2.4 ± 1.1%). These variations most probably did not arise as a result of changes in regional tracer distribution, but rather originated from the redrawing of ROIs for each SPECT investigation.

Stroke

Eighteen stroke patients (six female, 12 male, 23–75 yr of age; mean 48 ± 16.0 yr) were investigated. Seven suffered from transient ischemic attacks (TIA), three had a reversible ischemic neurologic deficit (RIND) and eight had a completed stroke (CS). Table 2 displays

TABLE 2
Cerebrovascular Disorders

		CAT positive	SPECT positive
CS	n = 8	7 (87.5%)	8 (100.0%)
RIND	n = 3	1 (33.3%)	3 (100.0%)
TIA	n = 7	3 (42.9%)	6 (85.7%)
Total	n = 18	11 (61.1%)	17 (94.4%)

Percentage of positive CAT and SPECT findings in 18 patients with cerebrovascular disease.

SPECT and CAT findings in these patients. Six of seven patients with TIAs had abnormal rCBF patterns revealed by SPECT, while in three of them CAT revealed a hypodense lesion. One patient with negative SPECT and CAT suffered from right-sided amaurosis fugax due to stenosis of the right internal carotid artery but had no motor or sensory disturbances. All patients with RIND had positive SPECT findings and one of them (Fig. 2) had a lesion (edema) which was visible by CAT. In this patient a control SPECT study showed normal tracer distribution 14 days after onset of symptoms. Two SPECT studies—before and after external carotid to internal carotid (EC-IC) bypass surgery—were obtained in another patient with a RIND (Fig. 3). In all eight patients with CS, SPECT showed impaired rCBF with seven of these patients also having positive CAT findings. In one CS patient SPECT revealed hyperperfusion 3 days following the stroke, whereas in a follow-up study 22 days later no luxury perfusion could be recognized. Technetium-99m HM-PAO SPECT revealed abnormal rCBF in 94% of stroke patients, while CAT revealed ischemic lesions in only 61% of these cases.

Epilepsy

Twenty-three seizure patients (eight female, 15 male, 16–60 yr of age; mean 35 ± 12.0 yr) were investigated by SPECT, (22 of them interictally and one during a postictal state (Fig. 4). CAT scans were available in 19. Table 3 shows the comparison between SPECT, CAT, and EEG results. Fourteen patients had partial complex seizures (PC) and nine patients had generalized seizures (GS). In the PC group 12 (86%) of 14 patients showed regionally decreased CBF mostly located in the temporal and frontotemporal region. CAT was abnormal in three instances, revealing small cysts in two patients and a presumed low grade astrocytoma in another patient. All EEG findings in the PC group were abnormal; six showed focal and six showed diffuse abnormalities. In four patients the site of the EEG focus corresponded well with the site of decreased rCBF detected by SPECT, while in two patients the SPECT focus was located contralaterally to that recorded by EEG. Seven of nine patients with GS had abnormal SPECT findings. In one patient, CAT showed a poren-

cephalic cyst and in another patient a cyst was located in the right lentiform nucleus. In this group EEG showed focal deficits in four patients, diffuse abnormalities in three patients and paroxysmal discharges in one patient. In this group, the site of the EEG and SPECT focus correlated well in all instances.

Extrapyramidal Disorders

SPECT was performed in seven patients with Parkinson's disease and in one patient with Huntington's chorea (four females, four males, 43–77 years of age; mean 55 ± 13.1 yr). In all Parkinsonian patients SPECT showed decreased cortical tracer deposition, without any regional preference. Low tracer uptake was also noted in the anterior basal ganglia either in one or both hemispheres in six instances. CAT revealed mild cortical atrophy in six patients and in one an internal and external hydrocephalus was detected. The SPECT study of one patient suffering from severe akinesia and rigidity is shown in Figure 5.

The patient who suffered from Huntington's disease for several years was a 46-yr-old female patient. In addition to severe dementia, aphasia was also present. One of her brothers also had the same disease. Low [^{99m}Tc]HM-PAO deposition was found in the left frontal, temporal and parietal cortex and no tracer uptake was seen in the anterior basal ganglia.

Dementia

Twelve patients (six females, six males, 52–82 yr of age; mean 63 ± 8.8 yr) with manifest signs of dementia were investigated. All of them had widened cortical sulci as demonstrated by CAT scanning. All SPECT studies showed an abnormal regional tracer distribution as well. Alzheimer's disease was assumed if low [^{99m}Tc]HM-PAO uptake was seen predominantly in the parietal and temporal lobes (Fig. 6). If disseminated areas of decreased tracer deposition, with no regional prevalence were found, then multi-infarct dementia was diagnosed. According to the tracer distribution patterns in SPECT images, four patients were classified as having Alzheimer's, one patient was classified as possibly being in the early stage of Alzheimer's dementia, one patient had a multi-infarct dementia, and five patients had

TABLE 3
Epilepsy: Percentage of positive CAT, SPECT, and EEG findings in 23 seizure patients.

		CAT n = 22 positive	SPECT n = 23 positive	EEG n = 19		
				Focus	Diffuse	Paroxysm
PC	n = 14	3 (23.1%)	12 (85.7%)	6 (50.0%)	6 (50.0%)	—
GS	n = 9	2 (22.2%)	7 (77.8%)	3 (42.9%)	3 (42.9%)	1 (14.2%)
Total	n = 23	5 (22.7%)	19 (82.6%)	9 (47.4%)	9 (47.4%)	1 (5.2%)

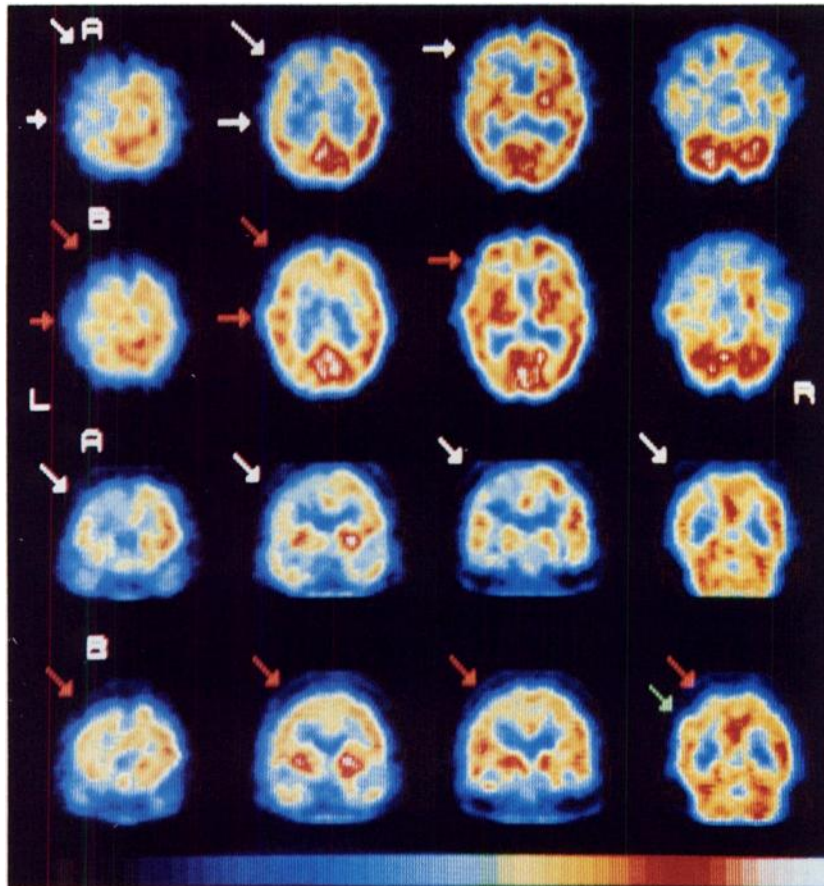


FIGURE 3

Transverse (first and second row; Cranial = left; caudal = right) and coronal (third and fourth row; frontal = left; occipital = right) cross-sections obtained in a 60-yr-old male patient with left sided TIAs and a RIND before (A) and (B) 14 days after EC-IC bypass-surgery. In (A) low tracer deposition is apparent in the left frontal and parietal lobe (white arrows). After bypass surgery (B) rCBF increased in these regions (red arrows) and the site of the anastomosis could be visualized (green arrow) (UHRES collimators).

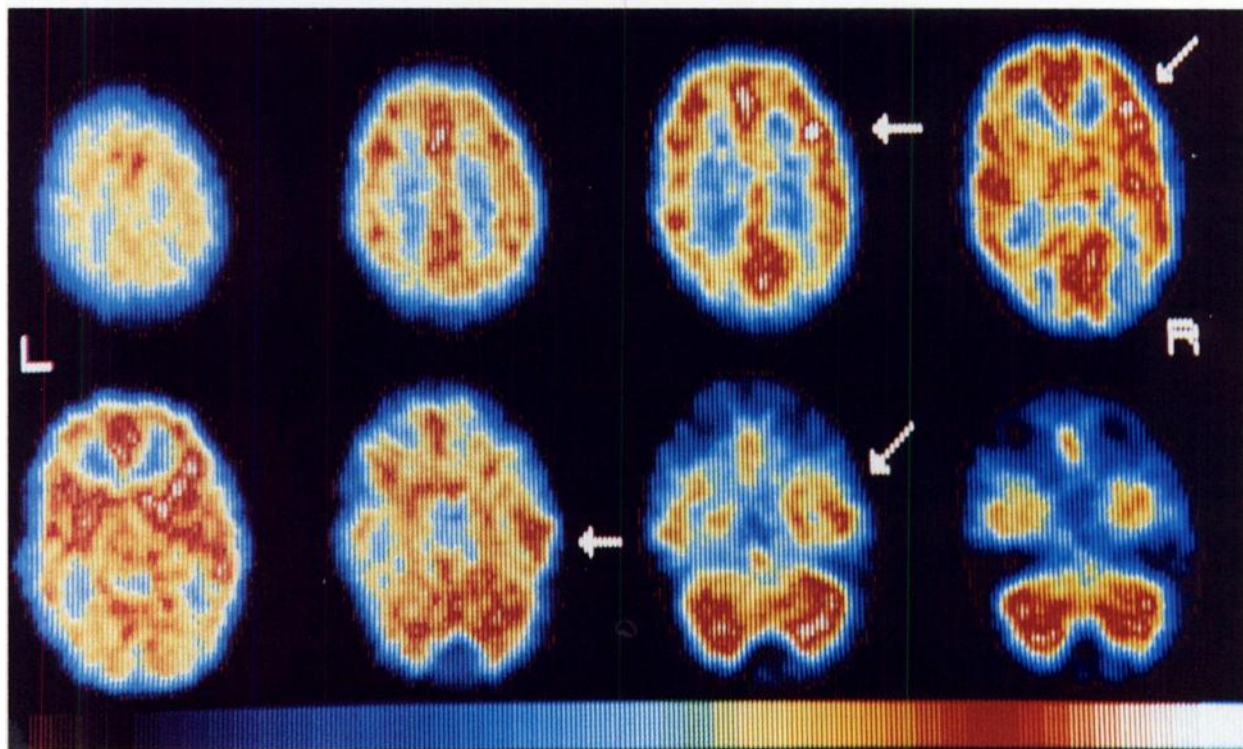


FIGURE 4

SPECT study obtained in a 20-yr-old male patient (cranial = left; caudal = right) in the postictal phase after a tonic-clonic seizure. Asymmetric rCBF is seen in the frontal (arrows in the top row) and temporal lobes (arrows in the bottom row), with the highest rCBF in the right medial and inferior frontal gyrus (arrows). At this time EEG revealed general paroxysmal discharges without focal signs. Three days later an EEG control showed a focus in the right temporoposterior region without paroxysms. The CAT scan was normal. (LEAP collimators).

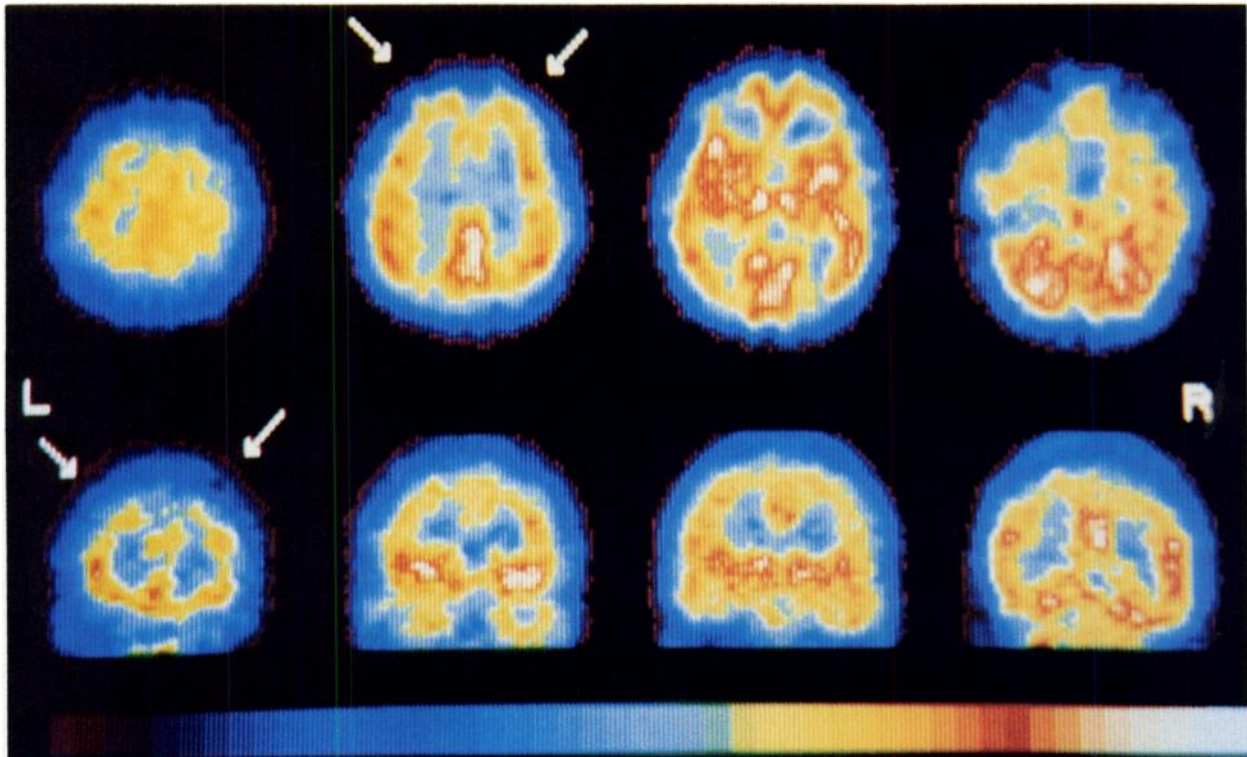


FIGURE 5
 Parkinson's disease: transverse cross sections (cranial = left; caudal = right) SPECT cross-sections obtained in a 43-yr-old male patient. Severe akinesia and rigidity were present. Slightly decreased tracer uptake in the superior frontal region (arrows) can be noticed. (HRES collimators).

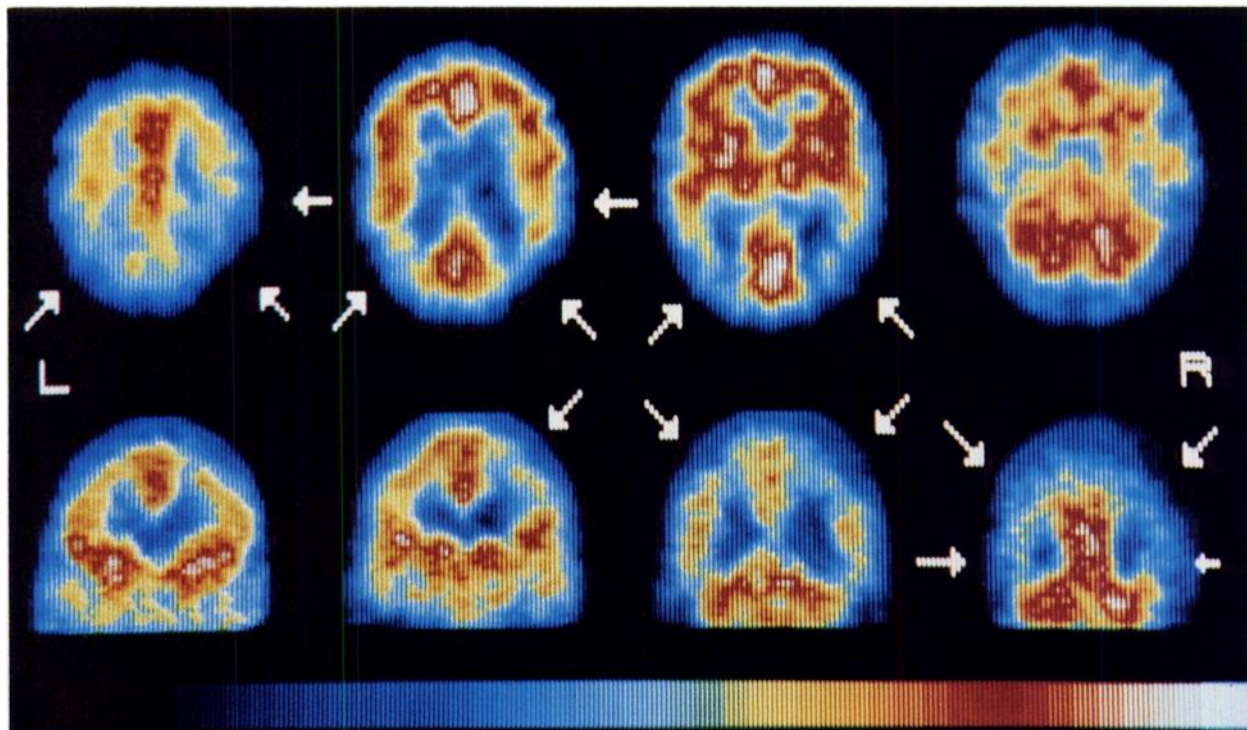


FIGURE 6
 SPECT study (transverse and coronal cross-sections; cranial = left; caudal = right; frontal = left; occipital = right) of a 60-yr-old male patient suffering from dementia of the Alzheimer type and supranuclear palsy (Steele-Richardson-Olchewsky syndrome). Symmetric decrease of rCBF is seen in the parietal and temporal lobes (arrows) (HRES collimators).

dementia of unknown type. Without knowledge of SPECT results one of the investigators performed neuropsychological examinations in six of these patients and independently came to the same diagnoses, namely four dementias of the Alzheimer type, one presumed early dementia of the Alzheimer type, and one nonclassifiable dementia.

Headache

Eleven patients suffering from headache (seven females, four males, 20–52 yr of age; mean 37 ± 10.8 yr) were examined. One had cluster headache, five had common migraine, and five had hemiplegic migraine. In two instances SPECT was performed during the attack (one patient with common migraine, one patient with hemiplegic migraine provoked by angiography). CAT scans were always normal. During the attack—free interval, SPECT findings were negative in the patient with cluster headache as well as two of the patients with common migraine and one of the patients with hemiplegic migraine. Positive findings were obtained in three patients with common migraine and in four patients with hemiplegic migraine. Here, a decreased tracer distribution was found, mostly located in the parietal and frontal cortex of one hemisphere. The two patients studied during an attack exhibited relatively low-perfused areas in the left parietal and left frontal cortex. In the patient with common migraine both superficial temporal arteries were clearly visible on SPECT images (Fig. 7).

Psychiatric Disorders

SPECT was performed in an heterogeneous group of 11 patients with psychiatric disturbances (eight female, three male, 21–64 yr of age; mean 35 ± 13.6 yr). Six patients suffered from paraphrenic syndrome, one had bipolar depression, one was classified as a borderline schizophrenic, one had anxiety, one had a compulsive disorder and one had panic attacks. The CAT scan was normal in eight patients, and in three patients minimal cortical atrophy was seen. In the group with paraphrenic syndrome, normal tracer distribution was seen in three instances, while three other patients showed decreased [^{99m}Tc]HM-PAO uptake in the frontal lobes, and in one of them, both central regions (Fig. 8). Two of these patients had high tracer concentrations in both hippocampi. The other five patients did not show any abnormality on SPECT images.

Neuropsychological Studies

Twenty-eight healthy male volunteers between 20 and 30 yr of age (mean 24 ± 2.3 yr) were investigated. Fourteen subjects listened through earphones to either low imagery sentences (e.g., “Austria has been a republic since 1918”) and the other 14 to high imagery sentences. Subjects had to judge whether the sentences

were correct or not. High imagery sentences contained motor actions (e.g., “To blow up the cheeks you have to close the mouth”) or of visual perceptions (e.g., “The green of pine trees is darker than that of grass”). Visual imagery led to a significant increase of the RIs in the inferior occipital region ($p = 0.035$ two tailed) and in both thalami ($p < 0.05$) when compared with the low imagery task. Particularly the finding of an activation of the left inferior occipital lobe in visual imagery is in good accord with previous clinical and experimental investigations concerning the neurological basis of imagery (13,14).

DISCUSSION

The principle interest of neurologists in emission computerized tomography (ECT) is the detection and visualization of metabolic or CBF changes in normal or “apparently normal” brain tissue.

With the development of iodine-123- (^{123}I) labeled compounds for the visualization of CBF N-isopropyl(^{123}I)-p-iodoamphetamine (15) or [^{123}I]HIPDM (16)] using SPECT, interest was broadened regarding this technique. Several authors have discussed its clinical utility in the detection of cerebrovascular disease (17), epileptogenic foci (18,19), other neurologic disorders (20) and in stimulation studies (14).

However, the relatively high costs and general unavailability of ^{123}I -labeled compounds has created the need for a ^{99m}Tc -labeled CBF-tracer that would remain trapped in brain tissue at a constant concentration for several hours. Technetium-99m HM-PAO has largely fulfilled these requirements. The extraction fraction of the tracer is ~80% with steady-state conditions being reached 2 to 3 min after injection (11). As shown in Figure 1 no redistribution between gray and white matter was observed during the first 2 hr after tracer administration. The ratio between these tissue components was 2.0. The relatively high counting rate and the easy availability of the tracer enabled us to obtain easily images of CBF in acute neurologic states such as an epileptic seizure or immediately thereafter in the post-ictal phase.

Should SPECT become a widely used clinical tool for the investigation of pathophysiologic mechanisms of brain disease and the confirmation of PET results in larger patient samples, several features should serve to support the extended use of this technique: (a) low investigation costs, due to the usage of standard equipment such as rotation scintillation cameras and tracers labeled with noncyclotron dependent isotopes; (b) spatial resolution allowing for the accurate recognition of cortical and subcortical structures; and (c) its high counting rates allowing for improved signal/noise ratios and avoidance of statistical artifact in the evaluation of SPECT studies.

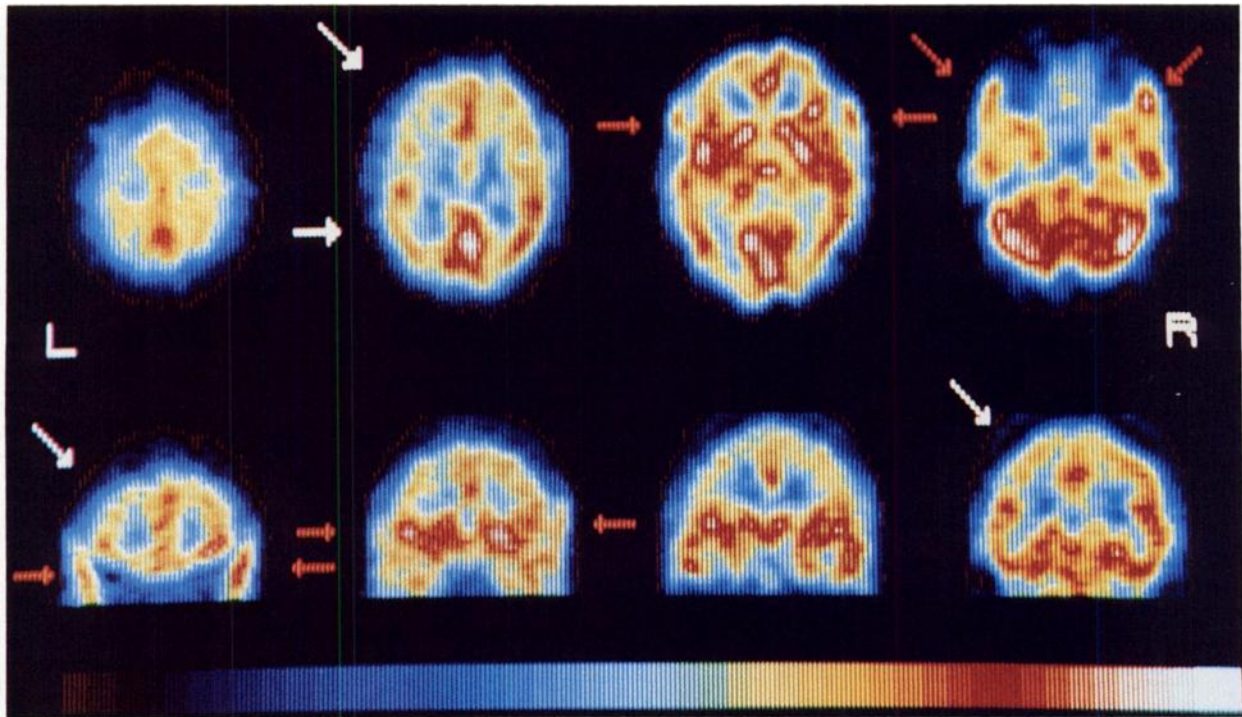


FIGURE 7
 SPECT study (transverse and coronal cross-sections; cranial = left; caudal = right; frontal = left; occipital = right) during an acute attack of common migraine in a 44-yr-old female patient. Relatively low tracer deposition in the left frontal and parietal lobe is visible (white arrows). The superficial temporal artery on both sides can be recognized (red arrows) (LEAP collimators).

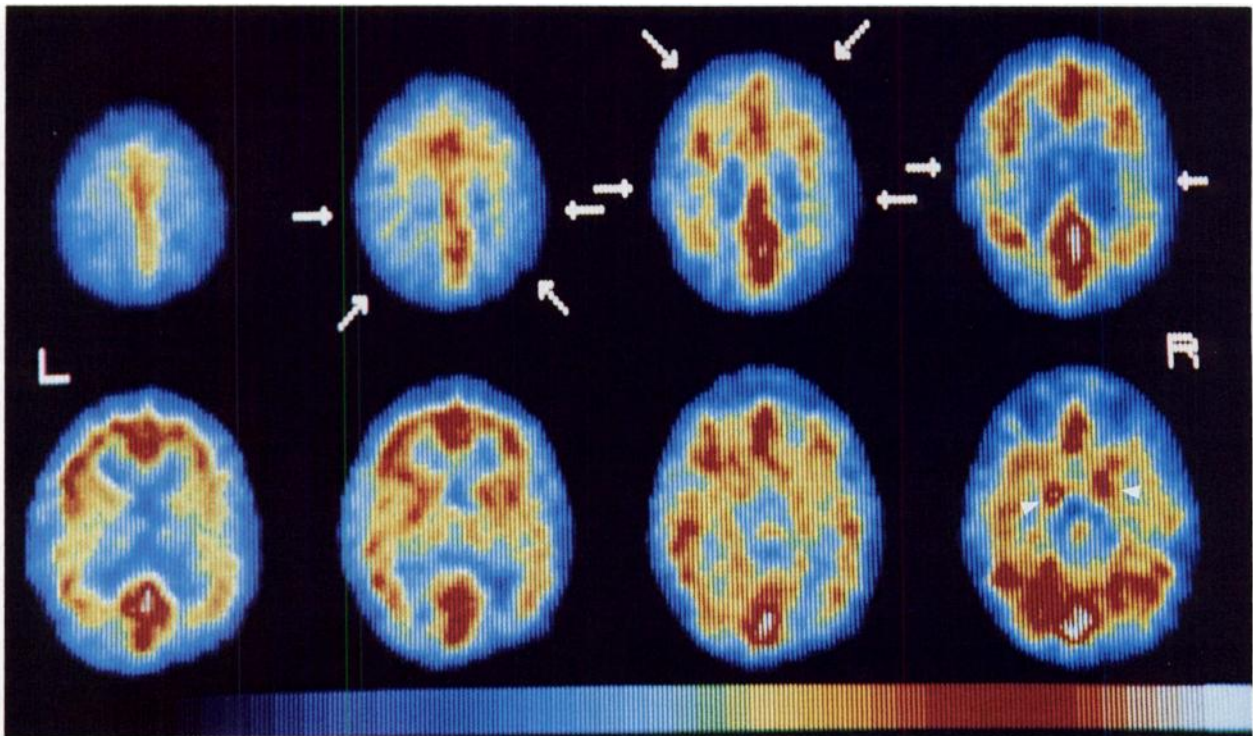


FIGURE 8
 SPECT study during auditory hallucinations in a 21-yr-old female patient (cranial = left; caudal = right). Note low tracer uptake in the central and parietal regions of both hemispheres (arrows) and high isotope concentration in both hippocampi (see arrows in the bottom right transverse section) (HRES collimators).

Since the biodistribution and kinetics of [^{99m}Tc]HM-PAO remain unclear, rCBF can not be expressed in absolute flow units at present. Therefore, in addition to visual estimation of SPECT images, we rely upon side to side differences of activity distribution in homologous brain regions. The regional [^{99m}Tc]HM-PAO distribution found in normal subjects compares well with results obtained in animals and in men with tracers showing CBF or glucose metabolism. Based upon these data, side to side differences above 12% were considered as pathologic.

Our results show [^{99m}Tc]HM-PAO SPECT to be very sensitive for detection of brain ischemia in transient or persistent perfusion deficits. Ischemic brain areas were seen in 94% of our stroke patients and changes of rCBF in the same patient at different disease stages could be recorded. In 83% of patients with epilepsy relatively decreased rCBF was found.

It is well known from PET studies that local metabolic impairment is more frequently seen in patients with partial complex rather than in generalized seizures. This agrees with our experience. However, the incidence of abnormally perfused regions in our patients with generalized seizures (78%) is rather high. Engel et al. (21) did not observe any regional impairment of glucose metabolism in patients suffering from generalized seizures during the inter-ictal phase. This discrepancy could arise from either differences in patient population or differences in spatial resolution between our system and the ECAT II scanner. Alternatively, our evaluation method could be in error (i.e., comparison of side/side differences in mean count rates/voxel in ROIs—versus calculation of rCMRglu in absolute units) if one assumes that rCBF and rCMRglu are proportionally impaired in these patients. In addition to hypoperfused regions, focal hyperperfusion was detected in a patient several hours after a tonic clonic seizure, in a state of psychomotor agitation, with impaired consciousness and with generalized paroxysms in the EEG. The sites of EEG foci compared well with the locations of SPECT changes, except in two patients with focal seizures. This could have been due to the well-known fact that epileptic foci in the EEG can project contralaterally (22).

Rigidity and akinesia were the predominant symptoms in patients suffering from Parkinson's disease. No specific tracer distribution pattern was observed. Decreased isotope deposition was seen either in cortical structures or in the anterior basal ganglia without any regional prevalence. This is in agreement with PET data in which a mild or moderate reduction of cortical glucose consumption was found in patients with bilateral parkinsonism (23) or decreased rCBF was seen in cases with hemiparkinsonisms (24,25).

Among the demented patients a typical tracer distribution was found in those suffering from Alzheimer's disease and one patient with Huntington's disease.

While Alzheimer patients showed decreased rCBF predominantly in the parietal and temporal lobe, the patient with Huntington's chorea had moderately decreased cortical tracer uptake and clearly impaired rCBF in the caudate nuclei similar to that observed previously in PET studies (26).

The asymmetries in rCBF observed during a hemiplegic migraine attack—with hypoperfusion contralateral to clinical symptoms—corresponded well to findings reported by Lauritzen et al. (27) using the intracarotid xenon-133 (¹³³Xe) clearance technique or ¹³³Xe SPECT. The clear visualization of extracranial vessels in one patient during a common migraine attack could represent vessel dilatation or tracer uptake in the vessel wall (edema?), since we have never seen such isotope concentration in the superficial temporal artery in any other [^{99m}Tc]HM-PAO SPECT study.

As the findings in some patients during hallucinations and in normal volunteers during imagery tasks revealed, specific regional brain activity can be visualized by [^{99m}Tc]HM-PAO SPECT. Electrical stimulation of the amygdaloid nucleus or hippocampus can provoke seizures as well as hallucinations (28). Confirming our theoretical expectations, we observed high tracer deposition in the hippocampi during acoustic hallucinations, in certain instances and in the occipital region during imagery tasks (13). At present, further investigations and statistical evaluations are in progress in order to substantiate our preliminary results reported here.

NOTES

* (Siemens Dual Rota ZLC 37) Searle-Siemens Medical Systems, Inc., Iselin, NJ.

† Nodecrest Micas 2000.

REFERENCES

1. Kung HF, Molnar M, Billings J, et al. Synthesis and biodistribution of neutral lipid-soluble Tc-99m complexes that cross the blood-brain barrier. *J Nucl Med* 1984; 25:326-332.
2. Holm S, Andersen AR, Vorstrup S, et al. Dynamic SPECT of the brain using a lipophilic technetium-99m complex, PnAO. *J Nucl Med* 1985; 26:1129-1134.
3. Neirinckx RD, Nowotnik DP, Pickett RD, et al. Development of a lipophilic Tc-99m complex useful for brain perfusion evaluation with conventional SPECT imaging equipment. In: Amphetamines and pH-shift agents for brain imaging: basic research and clinical results. Berlin—New York: Walter de Gruyter, 1986: 59-70.
4. Holmes RA, Chaplin SB, Royston KG, et al. Cerebral uptake and retention of 99Tcm-hexamethyl-propyleneamine oxime (99Tcm—HM-PAO). *Nucl Med Commun* 1985; 6:443-447.
5. Larsson SA, Bergstrand H, Bergstedt H, et al. A special cut off camera for high resolution SPECT of the head. *J Nucl Med* 1984; 5:1023-1030.

6. Polak JF, Holman BL, Moretti JL, et al. I-123 HIPDM brain imaging with a rotating gamma camera and slant-hole collimator. *J Nucl Med* 1984; 25:495-498.
7. Todd-Pokropek A, Di Paola R. The use of computers for image processing in nuclear medicine. *IEEE Trans Nucl Sci* 1982; 21:1299-1309.
8. Bellini S, Piacentini M, Cafforio C, et al. Compensation of tissue absorption in emission tomography. *IEEE Trans Acous Speech and Sign Proc ASSP* 1979; 27:213-218.
9. Madsen MT, Park ChH. Enhancement of SPECT images by Fourier filtering the projection image set. *J Nucl Med* 1985; 26:395-402.
10. King MA, Schwinger RB, Doherty PW, et al. Two-dimensional filtering of SPECT images using the Metz and Wiener filters. *J Nucl Med* 1984; 25:1234-1240.
11. Sharp PF, Smith FW, Gemmell HG, et al. Technetium-99m HM-PAO stereoisomers as potential agents for imaging regional cerebral blood flow: human volunteer studies. *J Nucl Med* 1986; 27:171-177.
12. Mazziotta J, Phelps ME, Plummer D, et al. Quantitation in positron emission computed tomography: 5. Physical-anatomical effects. *J Comput Assist Tomogr* 1981; 5:734-743.
13. Farah MJ. The neurological basis of mental imagery: a componential analysis. *Cognition* 1984; 18:245-272.
14. Goldenberg G, Podreka I, Steiner M, et al. Patterns of regional cerebral blood flow related to meaningfulness and imaginability of words—an emission computer tomography study. *Neuropsychologia* 1987; in press.
15. Winchell HS, Horst WD, Braun L, et al. N-isopropyl-(123)p-iodoamphetamine: single—pass brain uptake and washout; binding to the brain synaptosomes; and localisation in dog and monkey brain. *J Nucl Med* 1980; 21:947-952.
16. Kung HF, Trampusch KM, Blau M. A new brain perfusion imaging agent: 123I-HIPDM (N,N,N'-trimethyl-N'-2-hydroxy-3-methyl-5-iodobenzyl-1,3-propanediamine). *J Nucl Med* 1983; 24:66-72.
17. Hill RC, Magistretti PL, Holman BL, et al. Assessment of regional cerebral blood flow (rCBF) in stroke using SPECT and N-isopropyl-(I-123)-p-iodoamphetamine (IMP). *Stroke* 1984; 15:40-45.
18. Magistretti PL, Uren R, Shomer D, et al. Emission tomographic scans of cerebral blood flow using I123-iodoamphetamine in epilepsy. In: Proc. III. World Congr. Nucl. Med. & Biol. Paris: Pergamon Press, 1982: 139-143.
19. Kreiten K, Biersack HJ, Froescher W, et al. Erste Erfahrungen mit der "single-photon-emission computed tomography" (SPECT) des Gehirns bei Patienten mit Epilepsie. *Akt Neurol* 1985; 12:8-12.
20. Podreka I, Hoell K, Dal-Bianco P, et al. Klinische und technische Aspekte der SPECT-Hirnszintigraphie mit 123J-N-isopropyl-amphetamin. *NucCompact* 1984; 15:305-314.
21. Engel J. Metabolic patterns of human epilepsy: clinical observations and possible physiological correlates. In: Current problems in epilepsy. London: Paris: John Libbey Eurotext, 1983; 6-18.
22. Wieser HG, Meles HP, Bernoulli C, et al. Clinical and chronotopographic psychomotor seizure patterns. (SEEG study with reference to postoperative results). *Acta Neurochirurgica* 1980; 30(suppl):103-112.
23. Kuhl DE, Metter EJ, Riege WH. Patterns of local cerebral glucose utilisation determined in Parkinson's disease by the (18F) fluorodeoxyglucose method. *Ann Neurol* 1984; 15:419-424.
24. Perlmutter JS, Raichle ME. Regional blood flow in hemiparkinsonism. *Neurology* 1985; 35:1127-1134.
25. Wolfson LI, Leenders KL, Brown LL, et al. Alterations of regional cerebral blood flow and oxygen metabolism in Parkinson's disease. *Neurology* 1985; 35:1399-1405.
26. Metter EJ, Riege WH, Kameyama M, et al. Cerebral metabolic relationships for selected brain regions in Alzheimer's, Huntington's, and Parkinson's diseases. *J Cerebr Blood Flow & Metabol* 1984; 4:500-506.
27. Lauritzen M, Olsen TS, Olesen J, et al. Cerebral blood flow in migraine. *J Cerebr Blood Flow & Method* 1983; 3(suppl. 1):S63-S64.
28. Gloor P, Olivier A, Quesney LF, et al. The role of the limbic system in experiential phenomena of temporal lobe epilepsy. *Ann Neurol* 1982; 12:129-144.